Electronic Supplementary Material (ESI) for RSC Advances.

Supporting Information for "Understanding the Role of Cu^{+}/Cu^{0} Sites at Cu_2O Based Catalysts in Ethanol Production from CO_2 Electroreduction -A DFT Study"

Liren Sun,[a] Jinyu Han,[a] Qingfeng Ge,[a,b] Xinli Zhu,[a] and Hua Wang*[a]

[a.]Collaborative Innovation Center of Chemical Science and Engineering, Key Laboratory for Green Chemical Technology, School of Chemical Engineering and Technology, Tianjin University, Tianjin 300350, China.

[b.]Department of Chemistry and Biochemistry, Southern Illinois University, Carbondale Illinois 62901, United States.

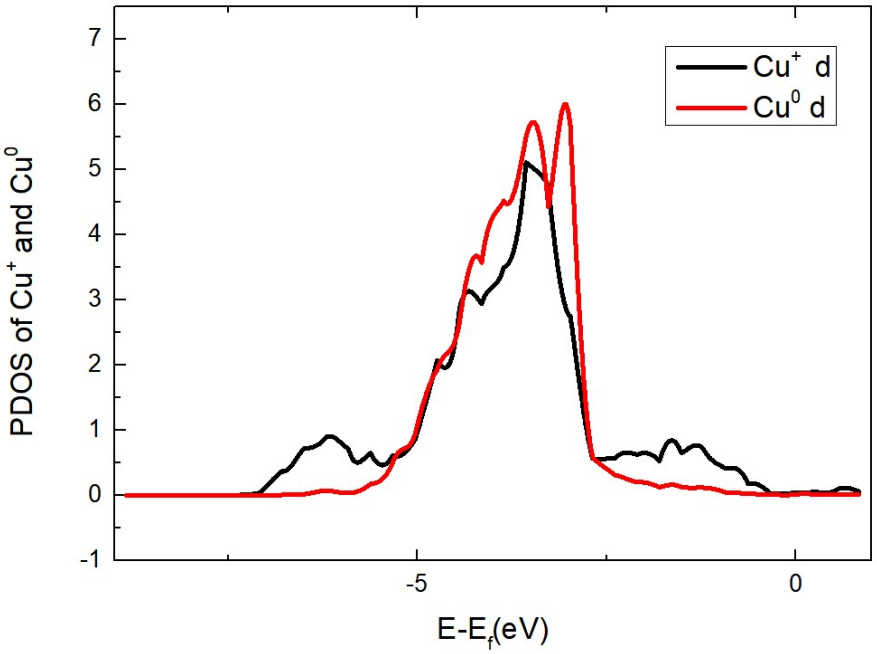

Fig. S1 Projected density of states (DOSs) of Cu^0 atom (red line) and Cu^+ atom (black line) in structure $Cu_{32}O_8(100)$.

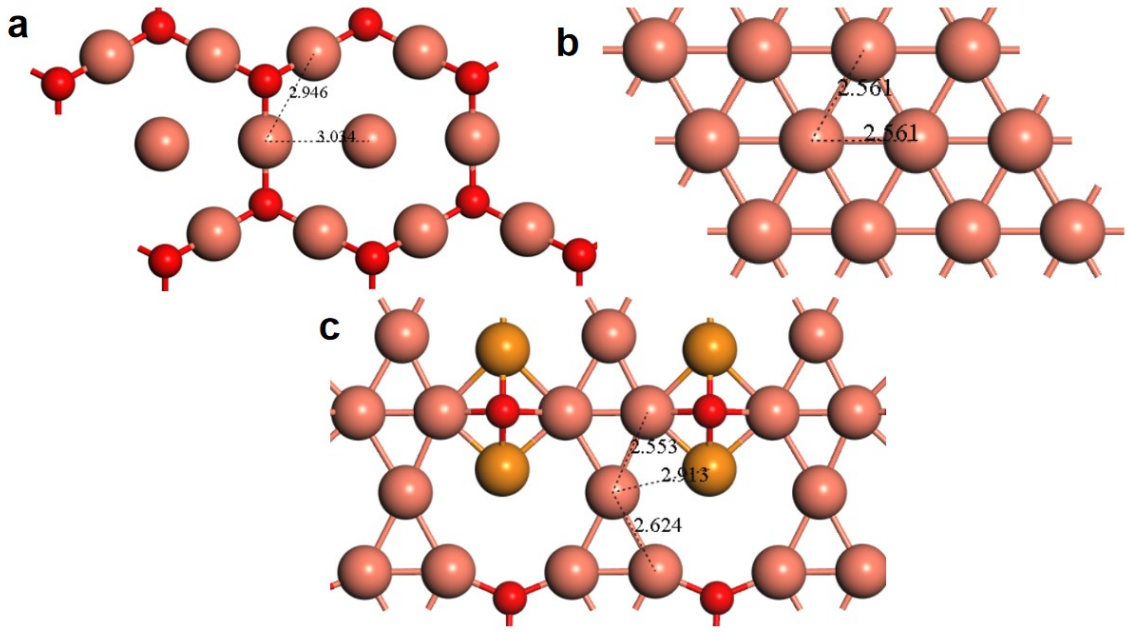

Fig. S2 The configuration of (a) $Cu_2O(111)$ surface (b) Cu(111)surface (c) Cu^+/Cu^0 surface. Distances between Cu atoms are marked. (Cu atoms are in orange red and O atoms are in red, Cu^+ atoms in (c) are in orange).

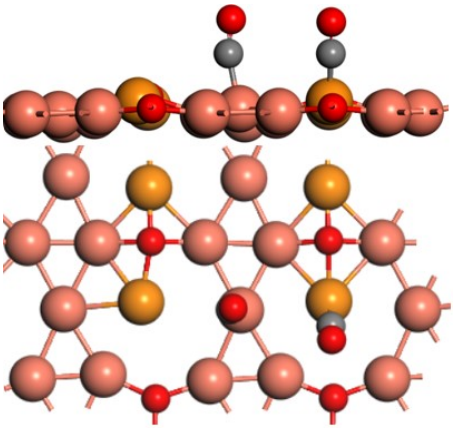

Fig. S3 The configuration of two *CO intermediates on Cu^{+} and Cu^{0} sites.

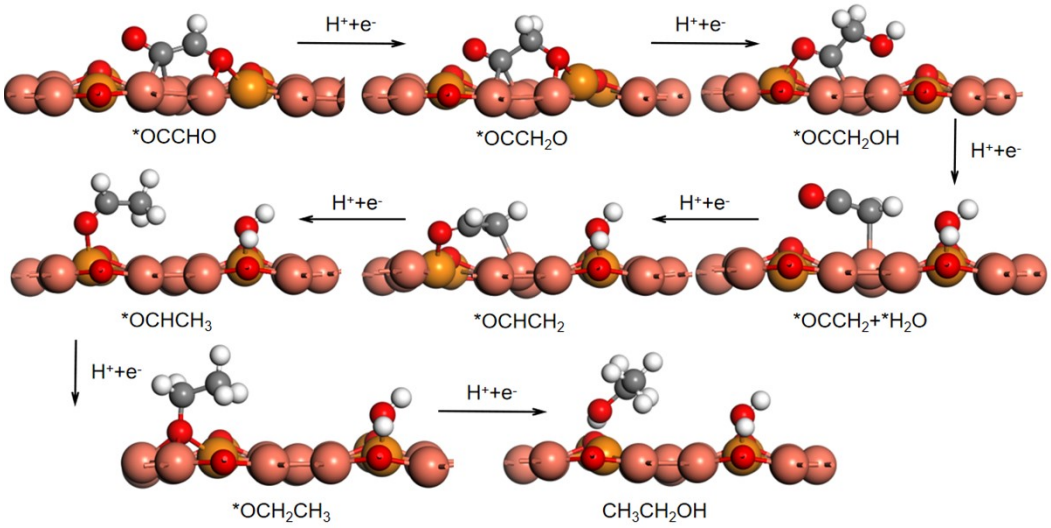

Fig. S4 The configuration of reaction intermediates for the later reduction of *OCCHO to ethanol.

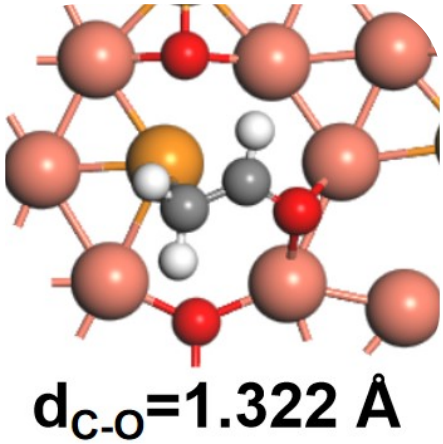

Fig. S5 Configuration of *$OCHCH_2$ with O atom combining to the Cu^{0} site.

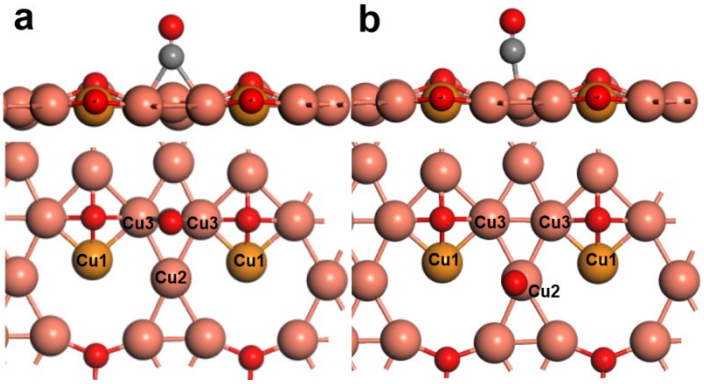

Fig. S6 (a) The structure of CO adsorbing on Cu3 atoms before optimization. (b) The structure after optimization of CO adsorbing on Cu3 atoms.

As shown in Fig S6, though we set a relative short distance between the CO and Cu3 atom in the initial configuration, as a result, CO adsorbs on the Cu2 atom in the final configuration after the optimization calculations. Cu3 atoms are not the crucial active sites in the adsorption of CO.

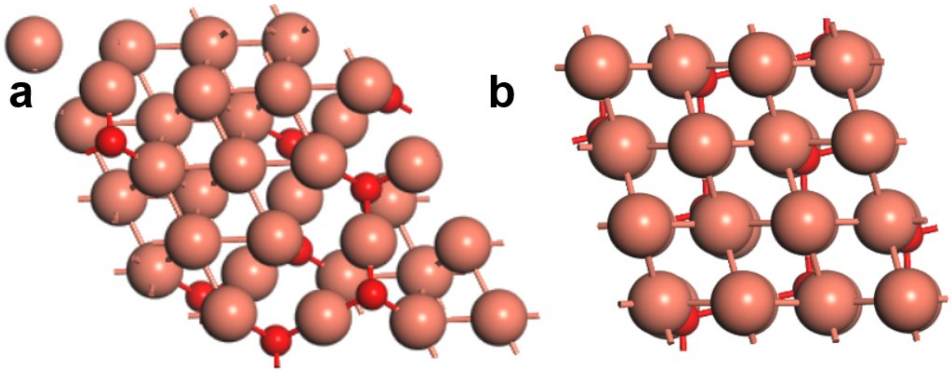

Fig. S7 Top surface of (a) $Cu_{32}O_8$ (111) and (b) $Cu_{32}O_8$ (010) facet.

Table S1. Free energy contributions for molecules at 298.15K.

Molecule	E_{elec} (eV)	ZPE (eV)	-TS (eV)	G (eV)	$G-E_{elec}$ (eV)
CO	-14.797	0.142	0.611	-15.266	-0.469
H_2O	-14.224	0.566	0.581	-14.239	-0.015
C_2H_4	-31.571	1.358	0.684	-30.897	0.674
C_2H_5OH	-46.933	2.113	0.874	-45.694	1.239
CH_3CHO	-38.969	1.473	0.821	-38.317	0.652

Table S2. Calculated electronic energies and corresponding free energies of adsorbed intermediates on Cu^+/Cu^0 surface at 298.15 K

Species/Adsorbates	E_{elec} (eV)	ZPE (eV)	-TS (eV)	G (eV)	$G-E_{elec}$ (eV)
$Cu-Cu_2O$	-206.77	3.397	8.109	-211.48	-4.712
$^*CO(Cu^+)$	-222.03	3.208	8.402	-227.23	-5.194
$^*CO(TS)$	-221.65	3.149	8.167	-226.66	-5.017
$^*CO(Cu^0)$	-221.74	3.241	8.333	-226.83	-5.093
$^*CO+^*CO$	-237.55	3.353	8.307	-242.51	-4.954
$^*CO+^*CHO$	-240.26	3.609	8.438	-245.09	-4.830
$^*CO+^*COH$	-239.55	3.601	8.082	-244.03	-4.481
$^*OCCHO$	-240.48	3.678	8.245	-245.04	-4.566
$^*OCCOH$	-239.99	3.696	8.390	-244.68	-4.694
$^*OCCH_2O$	-244.74	3.999	8.284	-249.02	-4.285
$^*OCCH_2OH$	-248.45	4.306	8.321	-252.47	-4.015
$^*OCCH_2$	-252.93	4.530	8.392	-256.80	-3.862
$^*OCHCH_2$	-257.27	4.836	8.463	-260.89	-3.628
$^*OCHCH_3$	-261.13	5.110	8.515	-264.53	-3.405
$^*OCH_2CH_3$	-265.20	5.475	8.514	-268.24	-3.038
$^*HOCH_2CH_3$	-269.35	5.757	8.514	-272.11	-2.757
$^*OCCHOH$	-244.27	4.002	8.280	-248.55	-4.278
$^*HOCCHO$	-244.37	4.006	8.555	-248.92	-4.549
$^*HOCCH_2O$	-247.66	4.307	8.276	-251.63	-3.969
$^*HOCCH_2OH$	-251.45	4.616	8.280	-255.11	-3.664
$^*HOCCH_2$	-256.53	4.870	8.416	-260.07	-3.547
$^*OCCH_3$	-256.90	4.819	8.387	-260.47	-3.567
$^*HOCHCH_3$	-264.45	5.459	8.390	-267.38	-2.931
$^*O+C_2H_4$	-261.04	5.134	8.418	-264.32	-3.284
$^*OH+C_2H_4$	-265.05	5.385	8.446	-268.12	-3.061
$^*H_2O+C_2H_4$	-268.99	5.676	8.379	-271.69	-2.703

Table S3. Reaction energy and reaction free energy at 0V vs. RHE of adsorbate states calculated at 298.15 K on Cu^{+}/Cu^{0} surface.

Species/Adsorbates	State	ΔE (eV)	ΔG (eV)
*OCCHO	*OCCHO+7(H^{+}+e^{-})	0.00	0.00
*$OCCH_2O$	*$OCCH_2O$+6(H^{+}+e^{-})	-0.881	-0.600
*$OCCH_2OH$	*$OCCH_2OH$+5(H^{+}+e^{-})	-1.217	-0.665
*$OCCH_2$	*$OCCH_2$+*H_2O+4(H^{+}+e^{-})	-2.319	-1.614
*$OCHCH_2$	*$OCHCH_2$+*H_2O+3(H^{+}+e^{-})	-3.272	-2.333
*$OCHCH_3$	*$OCHCH_3$+*H_2O+2(H^{+}+e^{-})	-3.753	-2.591
*OCH_2CH_3	*OCH_2CH_3+*H_2O+(H^{+}+e^{-})	-4.451	-2.923
*$HOCH_2CH_3$	*$HOCH_2CH_3$+*H_2O	-5.221	-3.411
*HOCCHO	*HOCCHO+6(H^{+}+e^{-})	-0.415	-0.494
*OCCHOH	*OCCHOH+6(H^{+}+e^{-})	-0.512	-0.127
*$HOCCH_2O$	*$HOCCH_2O$+5(H^{+}+e^{-})	-0.427	0.171
*$HOCCH_2OH$	*$HOCCH_2OH$+4(H^{+}+e^{-})	-0.831	0.072
*$HOCCH_2$	*$HOCCH_2$+*H_2O+3(H^{+}+e^{-})	-2.531	-1.511
*$OCCH_3$	*$OCCH_3$+*H_2O+3(H^{+}+e^{-})	-2.904	-1.905
*$HOCHCH_3$	*$HOCHCH_3$+*H_2O+(H^{+}+e^{-})	-3.694	-2.058
*O+C_2H_4	*O+C_2H_4+*H_2O+2(H^{+}+e^{-})	-3.661	-2.379
*OH+C_2H_4	*OH+C_2H_4+*H_2O+(H^{+}+e^{-})	-4.301	-2.583
*H_2O+C_2H_4	C_2H_4+2*H_2O	-4.857	-2.731

Details about $Cu_{32}O_8$ bulk

We study the oxygen desorption progress by layer-by-layer manner, which is energetically more favorable than random deoxidation manner. In order to simulate the oxygen desorption from bulk CuO, four O atoms were removed each time from the initial cell of $(CuO)_{32}$ in the (111) plane. After 8 steps of deoxidation by following the layer-by-layer mode, 32 O atoms were removed, resulting in the Cu_{32}. Note that both volume and symmetry have changed during the reduction from monoclinic CuO to cubic Cu_2O and Cu. Therefore, after each step of oxygen desorption, we used SSW-NN method to reconstruct the CuO_x structure.

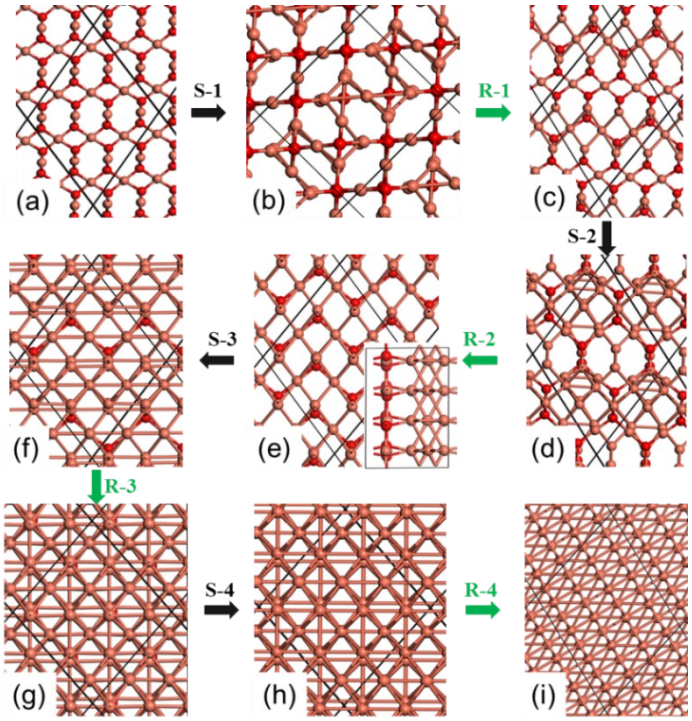

Fig. S8 Key structures following oxygen desorption in oxygen desorption at $C(O_v) \geq 50\%$. (a) $Cu_{32}O_{16}$ ($C(O_v) = 50\%$), (b, c) $Cu_{32}O12$ ($C(O_v) = 62.5\%$), (d, e) $Cu_{32}O_8$ ($C(O_v) = 75\%$), (f, g) $Cu_{32}O_4$ ($C(O_v) = 87.5\%$), and (h, i) Cu_{32} ($C(O_v) = 100\%$). The insert is a side view of the structure.

Fig. S8 shows the key structures following oxygen desorption in oxygen desorption at $C(O_v) \geq 50\%$ progress and the $Cu_{32}O_8$ bulk is shown in the Fig. S6d,e. Besides, by calculating the radial distribution functions (RDFs), which reflects the number of atoms at a given distance from a reference atom, we found two intense Cu-O peaks at 1.83 and 1.87 Å are present for $Cu_{32}O_8$ with $C(O_v)$ of 75% , which can be attributed to Cu_8O_8 phase. In the meantime, a sharp Cu-Cu peak at 2.79 Å is present. When $C(O_v)$ reaches 75% all oxygen atoms shift collectively towards b direction, resulting in an obvious phase separation. A clear phase interface is evident: one side is Cu_8O_8 phase while the other side is Cu_{24} phase. Therefore, the $Cu_{32}O_8$ structure is much more stable and more difficult to reduce.

Coordinates for $Cu_{32}O_8$ bulk and slab model structure

$Cu_{32}O_8$ bulk
1.0
9.0991001129 0.0000000000 0.0000000000
-0.1778604409 6.0615910772 0.0000000000
2.2222268721 -0.1050862992 8.8203621522
Cu O
32 8
Cartesian
4.711925030 2.634822369 5.721151829
5.236828327 1.379392982 7.879493713
6.867763042 4.525094509 5.668141365
5.150534153 4.501486778 7.873496056
9.179484367 2.613944530 5.657204151
2.960286140 2.613527298 7.900310516
2.323229313 4.430129051 5.671581268
7.492165089 2.629914284 7.888402462
4.680833817 0.259591371 5.654734135
7.561298370 0.254685462 7.898104668
6.954509735 1.405236006 5.674756050
2.929644108 0.237881362 7.833098888
9.249724388 0.239489034 5.668141365
9.703171730 4.405934334 7.875348568
2.404556513 1.493177176 5.675815105
9.786029816 1.466051698 7.881346703
3.520458460 2.667339563 1.246758223
6.399384499 2.663643599 3.490305424
5.762372017 4.484912872 1.261576414
6.368161678 0.288358301 3.423358917
8.151023865 2.688095331 1.310793996
4.042505264 4.458663464 3.464814663
1.207173586 4.580613136 1.257519007
8.589365959 4.553726196 3.463403225
3.589517355 0.292888165 1.257342696
8.675386429 1.431632042 3.469401121
5.844436169 1.544566393 1.265810132
4.125602245 1.518354416 3.470988750
8.120955467 0.312862992 1.244464993
1.900272369 0.308746129 3.487747669
1.294801712 1.459484816 1.263869643
1.831668854 2.683859110 3.477604151
3.349042416 4.486788750 8.242275238
6.951290131 4.466311932 7.503570080

9.620723724 4.465140820 6.039919376
7.563853741 4.501021385 0.891474009
3.960847139 4.518775463 1.629738331
4.124742031 4.447511673 5.301390648
6.787928581 4.538000107 3.831918001
1.290987372 4.519958019 3.092418909

$Cu_{32}O_8$ (100) slab
1.0
12.1283998489 0.0000000000 0.0000000000
-0.1702180729 9.0950068557 0.0000000000
0.0000000000 0.0000000000 17.3542995453
Cu O
64 16
Cartesian
1.175915837 4.098483086 2.621540546
-0.094334148 6.310570240 2.568262815
3.002179623 4.586157322 4.777985573
3.028934956 6.306023121 2.574857473
1.024011731 5.125400066 6.967230797
1.205971360 5.784606457 0.391339451
3.040571451 3.480931997 0.369125932
1.089450717 6.878008366 4.787877560
4.866919994 4.009442806 2.539975166
4.777401924 6.887285233 4.784927368
5.945281506 4.591341496 4.771738529
4.896500587 5.695020199 0.310468435
4.712784767 5.136132240 6.965147972
2.799896955 7.417068958 6.984931946
0.102533735 3.483842373 0.363225490
5.922987461 7.422071457 6.980072975
1.073179245 8.563949585 2.558717966
1.155218720 2.346511602 4.802108288
2.994427919 0.042837482 4.780068398
4.846110344 2.257016897 4.720716953
1.128321648 0.660115600 7.032482624
3.018684626 1.760156631 2.574683905
3.053420782 8.024069786 0.368084699
2.980244160 2.867928505 6.985452652
4.761964321 8.574045181 2.555593967
5.921299458 2.872294188 6.978510857
0.052990492 0.045929782 4.774861813
0.077207819 1.765340924 2.570171833
4.819197655 0.571439326 6.951959133

4.997524261	1.230372548	0.374332249
-0.068892077	8.029345512	0.362704873
1.309456348	1.220822811	0.377976626
7.240115643	4.098483086	2.621540546
5.969865322	6.310570240	2.568262815
9.066379547	4.586157322	4.777985573
9.093134880	6.306023121	2.574857473
7.088211536	5.125400066	6.967230797
7.270171165	5.784606457	0.391339451
9.104771614	3.480931997	0.369125932
7.153651237	6.878008366	4.787877560
10.931119919	4.009442806	2.539975166
10.841601372	6.887285233	4.784927368
12.009480476	4.591341496	4.771738529
10.960700035	5.695020199	0.310468435
10.776985168	5.136132240	6.965147972
8.864095688	7.417068958	6.984931946
6.166733742	3.483842373	0.363225490
11.987186432	7.422071457	6.980072975
7.137379646	8.563949585	2.558717966
7.219418526	2.346511602	4.802108288
9.058627129	0.042837482	4.780068398
10.910310745	2.257016897	4.720716953
7.192521572	0.660115600	7.032482624
9.082883835	1.760156631	2.574683905
9.117620468	8.024069786	0.368084699
9.044445038	2.867928505	6.985452652
10.826164246	8.574045181	2.555593967
11.985499382	2.872294188	6.978510857
6.117190361	0.045929782	4.774861813
6.141407967	1.765340924	2.570171833
10.883398056	0.571439326	6.951959133
11.061723709	1.230372548	0.374332249
5.995307446	8.029345512	0.362704873
7.373655796	1.220822811	0.377976626
3.067089796	6.224440575	0.738078356
2.940961838	6.386058807	4.409554005
2.861473083	5.617440224	7.354231834
2.957629442	0.123237349	6.617020607
2.910885096	9.055898666	2.944851160
3.005110979	3.561150074	2.206078529
3.017433882	2.786073446	5.148847103
3.160607100	0.728691936	0.000000000
9.131289482	6.224440575	0.738078356

9.005162239	6.386058807	4.409554005
8.925673485	5.617440224	7.354231834
9.021830559	0.123237349	6.617020607
8.975084305	9.055898666	2.944851160
9.069311142	3.561150074	2.206078529
9.081633568	2.786073446	5.148847103
9.224806786	0.728691936	0.000000000